



High critical current density and low anisotropy in textured $\text{Sr}_{1-x}\text{K}_x\text{Fe}_2\text{As}_2$ tapes for high field applications

Zhaoshun Gao¹, Yanwei Ma¹, Chao Yao¹, Xianping Zhang¹, Chunlei Wang¹, Dongliang Wang¹, Satoshi Awaji² & Kazuo Watanabe²

¹Key Laboratory of Applied Superconductivity, Institute of Electrical Engineering, Chinese Academy of Sciences, Beijing 100190, China, ²High Field Laboratory for Superconducting Materials, Institute for Materials Research, Tohoku University, Sendai 980-8577, Japan.

SUBJECT AREAS:
SUPERCONDUCTING
PROPERTIES AND
MATERIALS
CONDENSED-MATTER PHYSICS
MATERIALS SCIENCE
APPLIED PHYSICS

Received
4 October 2012

Accepted
23 November 2012

Published
19 December 2012

Correspondence and
requests for materials
should be addressed to
Y.M. (ywma@mail.iee.
ac.cn)

From the application point of view, large critical current densities J_c (H) for superconducting wires are required, preferably for magnetic fields higher than 5 T. Here we show that strong c -axis textured $\text{Sr}_{1-x}\text{K}_x\text{Fe}_2\text{As}_2$ tapes with nearly isotropic transport J_c were fabricated by an ex-situ powder-in-tube (PIT) process. At 4.2 K, the J_c values show extremely weak magnetic field dependence and reach high values of $1.7 \times 10^4 \text{ A/cm}^2$ at 10 T and $1.4 \times 10^4 \text{ A/cm}^2$ at 14 T, respectively, these values are by far the highest ever reported for iron based wires and approach the J_c level desired for practical applications. Transmission electron microscopy investigations revealed that amorphous oxide layers at grain boundaries were significantly reduced by Sn addition which resulted in greatly improved intergranular connectivity. Our results demonstrated the strong potential of using iron based superconductors for high field applications.

The discovery of superconductivity in the iron pnictides has generated a great deal of research interest, not only in basic physics, but also in the field of applied superconductivity^{1–7}. In addition to their high transition temperature, T_c , the Fe based superconductors were reported to have a rather high upper critical field, H_{c2} , and low H_{c2} anisotropy^{8–11}. Data reported so far has revealed many similarities between iron pnictide and cuprate superconductors, such as a layered crystalline structure and superconductivity induced by carrier doping. However, there are some distinct differences, such as a highly symmetric order parameter based on s+- wave in the iron pnictides compared to a d-wave pairing¹². Therefore, different characteristics of high-angle GBs can be expected. Indeed, Katase *et al.*¹³ performed a systematic study on the misorientation dependence of inter-grain J_c using an epitaxially grown Ba122 bi-crystal. The critical angle (θ_c) of the transition from a strong link to a weak link for Ba122 was found to be 9°, which is substantially larger than the value of 3–5° reported for YBCO. A remarkable transport inter-grain J_c of $\sim 10^5 \text{ A/cm}^2$ at 4 K and self field has been observed in samples of high misorientation angle of 45°. Such excellent properties suggest that the Fe based superconductors are promising for use in high magnetic field generation at liquid helium.

Earlier results indicate that the global critical current is limited by intergrain currents across grain boundaries in iron based superconductors^{13–21}. Some of which can be ascribed to extrinsic factors such as porosity, the amorphous phase at grain boundaries, and micro-cracks. Concerning the main intrinsic factor, J_c across the grain boundary decreases with grain boundary misorientation angle similar to that observed in the cuprates YBCO^{13,21}. In order to improve the grain connectivity of the iron based superconductors, a number of experimental techniques, including metal additions^{22–25}, rolling induced texture process^{26,28}, and hot isostatic press method²⁷, have been attempted. In this work, we report the further improvement of the transport critical current properties in textured $\text{Sr}_{0.6}\text{K}_{0.4}\text{Fe}_2\text{As}_2$ tapes with Sn additions. We observed a high transport critical current density of $> 10 \text{ kA/cm}^2$ at 4.2 K in 14 T field. Such a value is by far the highest ever reported for Fe based wires. The influences of Sn addition, microstructure, and the annealing process on achieving superior J_c properties will be discussed.

Results

The degree of grain texture was determined by XRD analysis. X-ray diffraction patterns of $\text{Sr}_{1-x}\text{K}_x\text{Fe}_2\text{As}_2$ bulk precursor, as-rolled tape, low temperature annealed tape, and high temperature annealed tape are shown

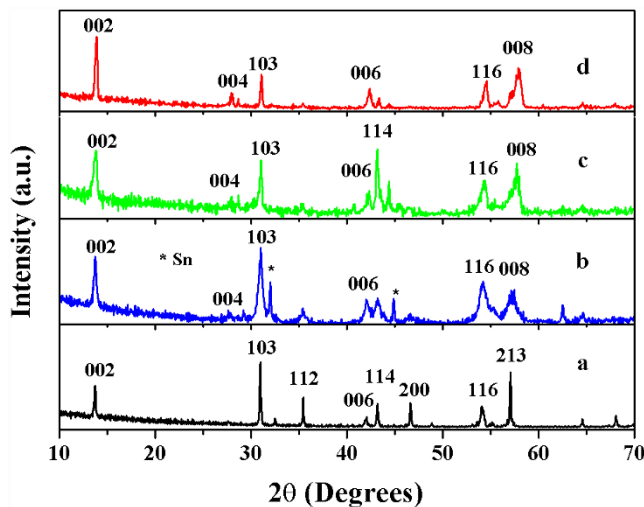


Figure 1 | X-ray diffraction patterns for $\text{Sr}_{1-x}\text{K}_x\text{Fe}_2\text{As}_2$ precursor bulk (a), as-rolled tape (b), tape annealed at low temperature (c) and tape annealed at high temperature (d).

collectively in Figure 1. The relative intensity of (103) peak with respect to that of (002) peak in all tape samples, when compared to the bulk precursor, is strongly reduced, indicating enhanced *c*-axis orientation. In order to have quantitative information about the texture of the $\text{Sr}_{1-x}\text{K}_x\text{Fe}_2\text{As}_2$ phase, we have evaluated the *c* axis orientation factor *F* by the Lotgering method as follows²⁹.

$$F = (\rho - \rho_0) / (1 - \rho_0),$$

Where $\rho = \sum I(00l) / \sum I(hkl)$, $\rho_0 = \sum I_0(00l) / \sum I_0(hkl)$, I and I_0 are the intensities of each reflection peak (hkl) for the oriented and random samples, respectively. The value of *F* for the as-rolled tape, was 0.316, the value of *F* for low temperature annealed tape was 0.348, and the value of *F* for high temperature annealed tape was 0.565, respectively. The cold deformation of the $\text{Sr}_{1-x}\text{K}_x\text{Fe}_2\text{As}_2$ tapes during the tape fabrication processes induces a relevant texture. In particular, the texture greatly improved after high temperature heat treatments.

Figure 2 presents the temperature dependent magnetic moment of samples measured in the magnetic field parallel to the *c*-axis. It is evident from the zero-field cooled (ZFC) signal that the diamagnetic signal does not saturate but continuous to decrease to lower temperature indicating some degrees of inhomogeneity in the sample annealed at high temperature. Note that low temperature annealing with longer time sharpens the T_c transition and reduces the

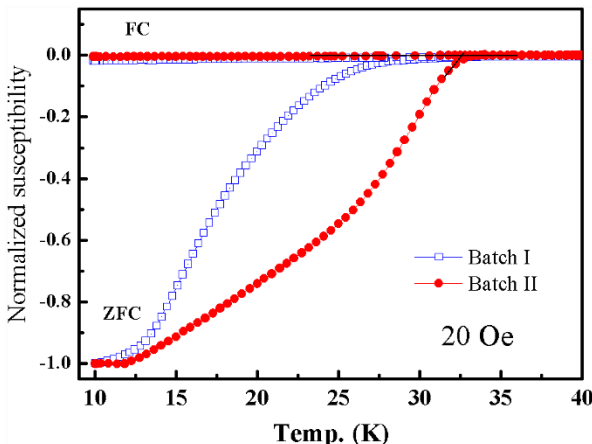


Figure 2 | Temperature dependence of magnetic susceptibility measured with field of 20 Oe for Batch I and Batch II samples.

inhomogeneities. Additionally, as shown more clearly in figure 2, low temperature annealing increased the onset T_c from 27.3 K to 32.5 K.

High critical current density in applied magnetic fields is essential for wire applications. Figure 3 shows the transport J_c measured as a function of applied magnetic fields along with reported values of other Fe-based superconducting wires and conventional Nb based superconducting wires^{25,27}. For the Batch II samples heated at low temperature, only data above 2 T are shown, because at lower field region, J_c is too high to be measured with our current apparatus. It can be seen that both samples demonstrate excellent J_c performance. Remarkably, the J_c of the tapes sintered at low temperature exhibits very weak field dependence and maintains a reasonably high value of $1.4 \times 10^4 \text{ A/cm}^2$ at 14 T, this J_c value is the highest ever reported for the iron based superconducting wires or tapes so far. It is about a factor of two higher than the best Ba-122 wire recently reported in ref. 27. Another interesting feature is the comparison of the superconducting properties of the present tapes with those of classical superconductors. The J_c value of $1.7 \times 10^4 \text{ A/cm}^2$ was achieved at 10 T for the tapes sintered at low temperature, which exceeded the value of NbTi conductors²⁵. To compare with the J_c of Nb₃Sn, the data above 14T for Batch II in Fig. 3 is extrapolated from low fields. As can be seen, a crossover with the J_c of Nb₃Sn would take place at around 19.5 T, as shown in figure 3. This indicates that the 122 superconducting wires may be competitive with well established Nb based conductors used in MRI and NMR for high field generation.

For application in superconducting magnets, low anisotropy in critical current (I_c) is more desirable. Figure 4 shows the $I_c(H//ab)$ and $I_c(H//c)$ dependences at 4.2 K for typical Batch I and II samples. It is even more striking that for both cases, I_c is larger when the applied field is perpendicular to the tape surface instead of along the *ab*-plane. Similar results were reported in several textured 122 films^{30–32}. In particular, in both of our samples, the anisotropy ratio of I_c ($\gamma = I_{c\perp}/I_{c\parallel} < 2$) appears to be much less than that in the cuprate superconductors. More interestingly, the I_c in Batch II tapes is nearly isotropic, which is a highly desirable property for high field applications.

Low magnification TEM images showed a grain boundary network in the textured $\text{Sr}_{0.6}\text{K}_{0.4}\text{Fe}_2\text{As}_2$ tapes, which are not shown here. The tape sample exhibits a layered structure with good alignment. Figure 5 (a) shows EDX line scan across one of grain boundary. Previous studies reported^{15,16,33} that the grain boundaries are usually coated by amorphous oxide layers. In contrast, we observed that the

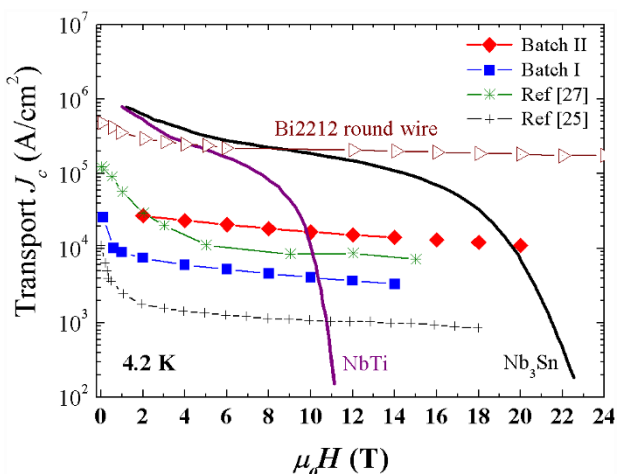


Figure 3 | The transport J_c values at 4.2 K obtained in this experiment plotted as a function of applied magnetic fields along with other Fe-based superconducting wires superconducting wires. The conventional Nb based and Bi2212 superconducting wires are also included for reference.

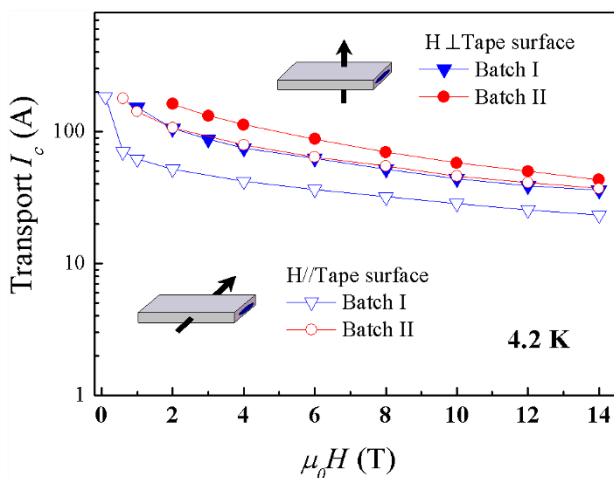


Figure 4 | Magnetic field dependence of I_c at 4.2 K for $\text{Sr}_{0.6}\text{K}_{0.4}\text{Fe}_2\text{As}_2$ tapes annealed at different temperatures. The magnetic field was applied parallel and perpendicular to the tape surface.

grain boundaries in Sn doped tapes are often filled with Sn rich materials (see fig. 5 (b)), note that the thickness of these interfaces are around 2–3 nm. Clearly, Sn and its alloy as flux can improve the crystallization of grain boundaries, diminish the formation of amorphous layer, and hence improve intergranular connectivity. In order to investigate the effect of annealing process on the tapes, we studied the difference in microstructures of the tapes heated at

different temperatures. Figure 5 (c) and (d) present scanning microscopy photomicrographs of Batch I and II tapes. Well-developed texture structures can be seen in both samples.

Discussion

As mentioned above, the J_c values of textured 122 pnictide tapes have reached over 10^4 A/cm^2 in a field of 14 T at 4.2 K. The well developed grain texture in our samples is a main reason for the superior J_c performance, since the misalignment in crystalline orientation at grain boundaries is a crucial weak-link in connectivity. Secondly, as shown by TEM study, Sn can promote the crystallization at grain boundaries, diminish the formation of amorphous layer, and hence much improved intergranular connectivity. Thirdly, low temperature synthesis results in highly dense material, which further contributes to good connectivity.

Our present results clearly show that textured Sr122 superconducting tapes, fabricated by the low-cost powder-in-tube process, exhibited extremely high and nearly isotropic transport J_c , as well as independent of the field behavior, demonstrating the potential for high field magnet applications. As the cumulative knowledge of pnictide PIT process grows, it is expected that the critical currents will continue to increase. We believe that the current PIT process can be applied industrially to fabricate high performance pnictide wires and tapes, as already demonstrated by the production of Bi-2223 and MgB_2 wires and tapes.

In summary, excellent transport J_c values under high magnetic field were observed in the textured $\text{Sr}_{1-x}\text{K}_x\text{Fe}_2\text{As}_2$ superconducting tapes that exhibit very small anisotropy. The well aligned superconducting grains and strengthened intergrain coupling achieved by

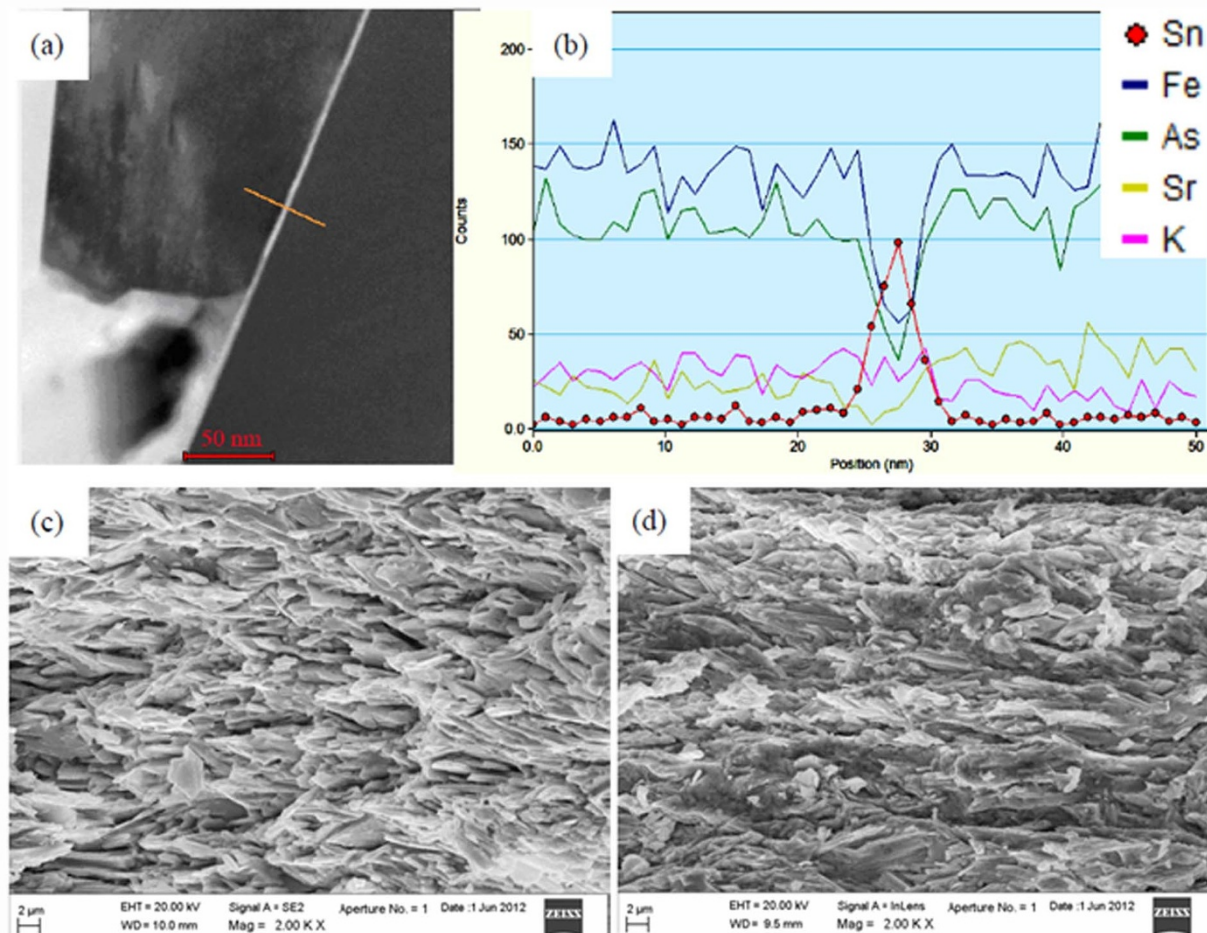


Figure 5 | (a) A STEM image of the $\text{Sr}_{0.6}\text{K}_{0.4}\text{Fe}_2\text{As}_2$ grain boundary. (b) The EDS line scan (as denoted in (a)) indicates that the grain boundary is filled with Sn rich material. Typical SEM images for $\text{Sr}_{0.6}\text{K}_{0.4}\text{Fe}_2\text{As}_2$ tapes annealed at high temperature (c) and low temperature (d).



Sn addition are responsible for this high J_c performance. With further improvement of critical current density and wire fabrication technology, use of $\text{Sr}_{1-x}\text{K}_x\text{Fe}_2\text{As}_2$ for very high field application is feasible.

Methods

Sample preparation. The $\text{Sr}_{1-x}\text{K}_x\text{Fe}_2\text{As}_2$ polycrystalline precursors were prepared by a one-step PIT method developed by our group²⁸. In order to compensate for loss of elements during the milling and sintering procedures, the starting mixture contains 10–20% excess K. The precursors were ground to a powder in an agate mortar and pestle. For Sn doped samples, 5–10 wt% Sn was added to the precursor powder and then the mixture was ground in a mortar for half an hour. The final powders were filled and sealed into an iron tube, which was subsequently swaged and drawn down to a wire of 1.9 mm in diameter. The as-drawn wires were then cold rolled into tapes (0.6 mm in thickness) with a reduction rate of 10–20%. The tapes were finally sintered following two different processes: sample was directly inserted into a furnace that was preheated to 1100°C, and removed from the furnace after 1–30 minutes (high temperature annealing process: Batch I), sample was sintered at 800–950°C for 1–30 minutes and then decreased to 600°C for 5 h (low temperature annealing process: Batch II).

Measurements. Phase integrity and texture of $\text{Sr}_{0.6}\text{K}_{0.4}\text{Fe}_2\text{As}_2$ grains were investigated using x-ray diffraction (XRD), for which iron sheath was mechanically removed after cutting the edges of the tape. Microstructure was studied using a scanning electron microscopy (SEM). DC magnetization measurements were carried out using a physical property measurement system (PPMS). The transport current I_c at 4.2 K and its magnetic field dependence were evaluated at the High Field Laboratory for Superconducting Materials (HFLSM) at Sendai, by standard four-probe method, with a criterion of 1 $\mu\text{V}/\text{cm}$, then the critical current was divided by the cross section area of the superconducting core to get the critical current density J_c . For each set of tapes, I_c measurement was performed on several samples to ensure the reproducibility.

1. Kamihara, Y. *et al.* Iron-based layered superconductor: $\text{La}[\text{O}_{1-x}\text{F}_x]\text{FeAs}$ ($x = 0.05–0.12$) with $T_c = 26$ K. *J. Am. Chem. Soc.* **130**, 3296–3297 (2008).
2. Chen, X. H. *et al.* Superconductivity at 43 K in $\text{SmFeAsO}_{1-x}\text{F}_x$. *Nature* **453**, 761–762 (2008).
3. Wen, H. H. *et al.* Superconductivity at 25 K in hole-doped $(\text{La}_{1-x}\text{Sr}_x)\text{OFeAs}$. *Europhys. Lett.* **82**, 17009 (2008).
4. Ren, Z. A. *et al.* Superconductivity at 55 K in iron-based F-doped layered quaternary compound $\text{Sm}[\text{O}_{1-x}\text{F}_x]\text{FeAs}$. *Chin. Phys. Lett.* **25**, 2215 (2008).
5. Rotter, M., Tegel, M. & Johrendt, D. Superconductivity at 38 K in the iron arsenide $\text{Ba}_{1-x}\text{K}_x\text{Fe}_2\text{As}_2$. *Phys. Rev. Lett.* **101**, 107006 (2008).
6. Prozorov, R. *et al.* Intrinsic magnetic properties of the superconductor $\text{NdFeAsO}_{0.9}\text{F}_{0.1}$ from local and global measurements. *New J. Phys.* **11**, 035004 (2009).
7. Hunte, F. *et al.* Two-band superconductivity in $\text{LaFeAsO}_{0.89}\text{F}_{0.11}$ at very high magnetic field. *Nature* **453**, 903–905 (2008).
8. Senatore, C. *et al.* Upper critical field well above 100 T for the $\text{SmFeAsO}_{0.85}\text{F}_{0.15}$. *Phys. Rev. B* **78**, 054514 (2008).
9. Yamamoto, A. *et al.* Small anisotropy, weak thermal fluctuations, and high field superconductivity in Co-doped iron pnictide $\text{Ba}(\text{Fe}_{1-x}\text{Co}_x)_2\text{As}_2$. *Appl. Phys. Lett.* **94**, 062511 (2009).
10. Putti, M. *et al.* New Fe-based superconductors: Properties relevant for applications. *Supercond. Sci. Technol.* **23**, 034003 (2010).
11. Yuan, H. Q. *et al.* Nearly isotropic superconductivity in $(\text{Ba}, \text{K})\text{Fe}_2\text{As}_2$. *Nature* **457**, 565–568 (2009).
12. Stewart, G. R. Superconductivity in iron compounds. *Rev. Mod. Phys.* **83**, 1589 (2011).
13. Katase, T. *et al.* Advantageous grain boundaries in iron pnictide superconductors. *Nature Commun.* **2**, 409 (2011).
14. Yamamoto, A. *et al.* Evidence for electromagnetic granularity in the polycrystalline iron-based superconductor $\text{LaO}_{0.89}\text{F}_{0.11}\text{FeAs}$. *Appl. Phys. Lett.* **92**, 252501 (2008).
15. Moore, J. D. *et al.* Evidence for supercurrent connectivity in conglomerate particles in $\text{NdFeAsO}_{1-\delta}$. *Supercond. Sci. Technol.* **21**, 092004 (2008).

16. Kametani, F. *et al.* Combined microstructural and magneto-optical study of current flow in polycrystalline forms of Nd and Sm Fe-oxypnictides. *Supercond. Sci. Technol.* **22**, 015010 (2009).
17. Gao, Z. *et al.* Superconducting properties of granular $\text{SmFeAsO}_{1-x}\text{F}_x$ wires with $T_c = 52$ K prepared by the powder-in-tube method. *Supercond. Sci. Technol.* **21**, 112001 (2008).
18. Wang, L. *et al.* Structural and critical current properties in polycrystalline $\text{SmO}_{1-x}\text{F}_x\text{FeAs}$. *Supercond. Sci. Technol.* **22**, 015019 (2009).
19. Qi, Y. *et al.* Superconductivity of powder-in-tube $\text{Sr}_{0.6}\text{K}_{0.4}\text{Fe}_2\text{As}_2$ wires. *Physica C* **469**, 717 (2009).
20. Mizuguchi, Y. *et al.* Fabrication of the iron-based superconducting wire using $\text{Fe}(\text{Se}, \text{Te})$. *Appl. Phys. Express* **2**, 083004 (2009).
21. Lee, S. *et al.* Weak-link behavior of grain boundaries in superconducting $\text{Ba}(\text{Fe}_{1-x}\text{Co}_x)_2\text{As}_2$ bicrystals. *Appl. Phys. Lett.* **95**, 212505 (2009).
22. Wang, L. *et al.* Large transport critical currents of powder-in-tube $\text{Sr}_{0.6}\text{K}_{0.4}\text{Fe}_2\text{As}_2/\text{Ag}$ superconducting wires and tapes. *Physica C* **470**, 183–186 (2010).
23. Wang, L. *et al.* Influence of Pb addition on the superconducting properties of polycrystalline $\text{Sr}_{0.6}\text{K}_{0.4}\text{Fe}_2\text{As}_2$. *Supercond. Sci. Technol.* **23**, 054010 (2010).
24. Togano, K., Matsumoto, A. & Kumakura, H. Large transport critical current densities of Ag sheathed $(\text{Ba}, \text{K})\text{Fe}_2\text{As}_2 + \text{Ag}$ superconducting wires fabricated by an *ex-situ* powder-in-tube process. *Appl. Phys. Express* **4**, 043101 (2011).
25. Togano, K., Matsumoto, A. & Kumakura, H. Fabrication and transport properties of ex situ powder-in-tube (PIT) processed $(\text{Ba}, \text{K})\text{Fe}_2\text{As}_2$ superconducting wires. *Solid State Commun.* **152**, 740 (2012).
26. Gao, Z. *et al.* High transport critical current densities in textured Fe-sheathed $\text{Sr}_{1-x}\text{K}_x\text{Fe}_2\text{As}_2 + \text{Sn}$ superconducting tapes. *Appl. Phys. Lett.* **99**, 242506 (2011).
27. Weiss, J. D. *et al.* High intergrain critical current density in fine-grain $(\text{Ba}_{0.6}\text{K}_{0.4})\text{Fe}_2\text{As}_2$ wires and bulks. *Nature Mater.* **11**, 682 (2012).
28. Wang, L. *et al.* Textured $\text{Sr}_{1-x}\text{K}_x\text{Fe}_2\text{As}_2$ superconducting tapes with high critical current density. *Physica C* **47**, 1689 (2011).
29. Lotgering, F. K. Topotactical reactions with ferrimagnetic oxides having hexagonal crystal structures-I. *J. Inorg. Nucl. Chem.* **9**, 113 (1959).
30. Tarantini, C. *et al.* Strong vortex pinning in Co-doped BaFe_2As_2 single crystal thin films. *Appl. Phys. Lett.* **96**, 142510 (2010).
31. Katase, T. *et al.* Biaxially textured cobalt-doped BaFe_2As_2 films with high critical current density over 1 MA/cm² on MgO-buffered metal-tape flexible substrates. *Appl. Phys. Lett.* **98**, 242510 (2011).
32. Trommler, S. *et al.* Architecture, microstructure and J_c anisotropy of highly oriented biaxially textured Co-doped BaFe_2As_2 on Fe/IBAD-MgO-buffered metal tapes. *Supercond. Sci. Technol.* **25**, 084019 (2012).
33. Wang, L. *et al.* Direct observation of nanometer-scale amorphous layers and oxide crystallites at grain boundaries in polycrystalline $\text{Sr}_{1-x}\text{K}_x\text{Fe}_2\text{As}_2$ superconductors. *Appl. Phys. Lett.* **98**, 222504 (2011).

Acknowledgements

The authors thank Drs. Qingxiao Wang and XiXiang Zhang at the KAUST for the TEM investigation. They are also indebted to Dr. Ma at ANL for useful suggestion. This work is partially supported by the National '973' Program (Grant No. 2011CBA00105) and National Natural Science Foundation of China (Grant No. 51002150 and 51025726).

Author contributions

Z.S.G. and C.Y. did most of the synthesis and characterizations. X.P.Z. and C.Y. did the heat treatment and in-field I_c measurement experiments. Z.S.G. and Y.W.M. wrote the paper. C.L.W., D.L.W., S.A. and K.W. helped with the experiment.

Additional information

Competing financial interests: The authors declare no competing financial interests.

License: This work is licensed under a Creative Commons

Attribution-NonCommercial-NoDerivs 3.0 Unported License. To view a copy of this license, visit <http://creativecommons.org/licenses/by-nc-nd/3.0/>

How to cite this article: Gao, Z. *et al.* High critical current density and low anisotropy in textured $\text{Sr}_{1-x}\text{K}_x\text{Fe}_2\text{As}_2$ tapes for high field applications. *Sci. Rep.* **2**, 998; DOI:10.1038/srep00998 (2012).